Single-Molecule Thermometry

DOI: 10.1002/anie.201310172

Yoctoliter Thermometry for Single-Molecule Investigations: A Generic Bead-on-a-Tip Temperature-Control Module**

*Deepak Koirala, Jibin Abraham Punnoose, Prakash Shrestha, and Hanbin Mao**

Abstract: *A new temperature-jump (T-jump) strategy avoids photo-damage of individual molecules by focusing a low-intensity laser on a black microparticle at the tip of a capillary. The black particle produces an efficient photothermal effect that enables a wide selection of lasers with powers in the milliwatt range to achieve a T-jump of 65°C within milliseconds. To measure the temperature in situ in single-molecule experiments, the temperature-dependent mechanical unfolding of a single DNA hairpin molecule was monitored by optical tweezers within a yoctoliter volume. Using this bead-on-a-tip module and the robust single-molecule thermometer, full thermodynamic landscapes for the unfolding of this DNA hairpin were retrieved. These approaches are likely to provide powerful tools for the microanalytical investigation of dynamic processes with a combination of T-jump and single-molecule techniques.*

Laser-induced temperature variation (T-jump)[1,2] and single-molecule techniques[3] are two invaluable methods to probe the dynamics of physiochemical and biochemical processes. However, these two techniques are not fully compatible with each other. The high-intensity laser pulses that are employed for T-jumps often cause photoinduced damage, such as photobleaching or a permanent change of conformation,[4] in a sample, particularly at the single-molecule level.[5] In conventional T-jump techniques, a rapid change in temperature is achieved by the photothermal effect of a specific laser on solvent or dye molecules or micro- or nanoobjects in the surroundings,[2,6,7] which necessitates a careful matching of the laser source and the heating material. To measure the temperature, observables, such as the fluorescence or photoluminescence of dye molecules, are often used. Nevertheless, these approaches are difficult to provide in situ temperature information without interfering with the system of interest. To reduce this interference, temperature profiles are often characterized before the experiments, which adds uncertainty to real-time temperature measurements. For single-molecule investigations, however, it is desirable to follow the temperature in situ and in real time as the transitions at this level are stochastic and highly dynamic. To the best of our knowledge, real-time and in situ temperature measurements have not been achieved in single-molecule T-jump experiments.

We noticed that during the mechanical unfolding of individual molecules, mechanical forces destabilize the chemical forces, such as hydrogen bonding or van der Waals interactions (the mechanochemical effect).[8] As the strength of a chemical force is dependent on temperature, this mechanochemical behavior is expected to be a function of temperature as well. With this hypothesis in mind, we herein describe a method for mechanochemistry-based thermometry, in which the temperature is monitored through the measurement of the unfolding force (F_{unfold}) of a single-molecule probe. As a proof of concept, we used a DNA hairpin structure (with a 10 base pair (bp) stem and a 15 nucleotide (nt) loop) as a single-molecule thermometer to measure the profile of a unique temperature-control bead-on-a-tip (BOAT) module. The mechanical unfolding and refolding of this hairpin is confined to a yoctoliter (10^{-24} L) volume, thus providing a spatial resolution that cannot be achieved with conventional thermometry.

The BOAT module was constructed by placing a particle with a diameter of 600 nm to 3 μm at the tip of a capillary (300–500 nm inner diameter) using suction (Figure 1a and c; see also the Supporting Information, Section S1 and Figure S1). A variety of black materials, such as carbon spheres and metallic and magnetic particles, which efficiently absorb light of a wide range of wavelengths, could be used as the bead. When a low-intensity laser is focused on the black particle, the highly efficient photothermal effect heats the bead, which leads to heating of the surroundings irrespective of the medium type (aqueous or organic). As the low-intensity laser is focused on the bead instead of the sample, photodamage is minimized.

To measure the temperature profile of the BOAT module using the mechanochemical properties of a single molecule, we placed the BOAT module close to the two optically trapped beads between which the DNA hairpin thermometer was tethered through affinity interactions (Figure 1b and c; see also Section S2–S4 and Figure S2). To reveal the relationship between the mechanical stability of the hairpin and the temperature, we first measured the rupture force, F_{unfold}, of the hairpin during the rupture event, which was observed in a force–extension (F–X) curve in the absence of laser illumination of the BOAT module. Whereas F_{unfold} represents the mechanical stability, the size of the rupture event is depicted by the change in contour length (ΔL, Figure 1d, "BOAT off"; see also Section S4). The observed F_{unfold} and ΔL were consistent with previous studies on similar DNA hairpins[9] (Section S4 and Figure S3). When a 532 nm laser (10 mW) was focused on the BOAT module, F_{unfold} of a hairpin

[*] D. Koirala, J. A. Punnoose, P. Shrestha, Prof. H. Mao
Department of Chemistry and Biochemistry
Kent State University
Kent, OH 44242 (USA)
E-mail: hmao@kent.edu

[**] We would like to thank the Ohio Board of Regents and the NSF (CHE-1026532) for financial support.

Supporting information for this article is available on the WWW under http://dx.doi.org/10.1002/anie.201310172.

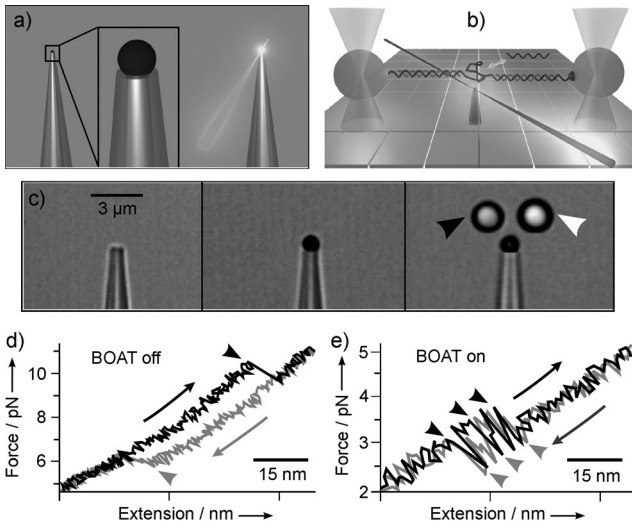

Figure 1. BOAT module and single-molecule mechanochemical thermometry. a) BOAT module. b) Experimental setup of the BOAT-integrated optical tweezers. c) Images of a capillary tip, a 1 μm BOAT module, and a BOAT module with two optically trapped beads. The black and white arrowheads indicate the beads that are coated with streptavidin (1.9 μm) and anti-digoxigenin antibody (2.1 μm), respectively. d, e) Typical stretching (——) and relaxing (——) force–extension curves of the hairpin located 1 μm away from the BOAT without (BOAT off; d) and with (BOAT on; e) laser illumination (10 mW, 532 nm). The unfolding and refolding processes of the hairpin are depicted by black and gray arrowheads, respectively.

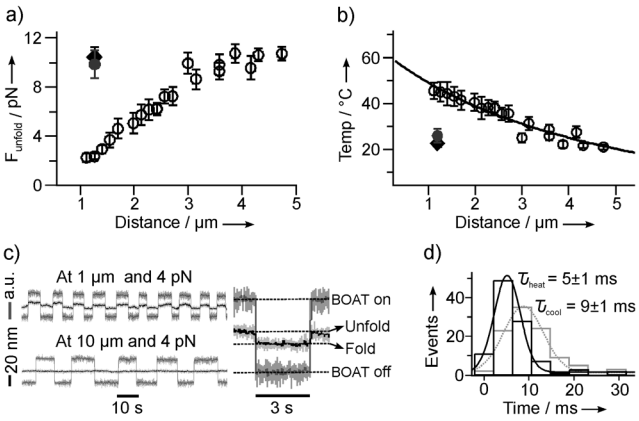

Figure 2. T-jump of the BOAT module measured by single-molecule mechanochemical thermometry. a) The unfolding force (F_{unfold}) of the DNA hairpin thermosensor at various locations away from the BOAT (○: BOAT on; ●: BOAT off; ◆: control). b) The temperature profile of the BOAT module (○) agrees well with the theoretical prediction (——). c) The top panel and the enlarged region (right) depict the time traces (——) of the folding or unfolding process of the DNA hairpin that is located 1 μm away from the BOAT module at 4 pN in response to the on or off state of the BOAT module, which is depicted by the laser intensity (——). Hopping of the hairpin that is located 10 μm away from the BOAT is not observed irrespective of the BOAT illumination (bottom). d) Histograms of the transition time (τ) for the heating (——, 5 ± 1 ms) and the cooling (——, 9 ± 1 ms) cycles of the BOAT module. The Gaussian curves are fitted to the histograms.

located 1 μm away from the BOAT decreased significantly (10.4 ± 0.3 vs. 3.4 ± 0.2 pN), whereas ΔL remained constant (Figure 1e, "BOAT on"; see also Section S5 and Figure S4). A control experiment in which a non-heating polystyrene particle was illuminated by the same laser did not show significant change in F_{unfold} (Section S5 and Figure S4), confirming that the decrease in F_{unfold} was solely due to the heat generated by the BOAT module. The unfolding–refolding processes and the hysteresis area between the stretching and returning F–X curves (Figure 1d, "BOAT off" and Figure 1e, "BOAT on") clearly demonstrated that the transition processes became faster when the BOAT was turned on by the 532 nm laser. These results reflect the unique and highly sensitive response of the DNA hairpin to the temperature variation.

To explore the potential of the DNA hairpin as a single-molecule thermometer, we first measured its unfolding force at different temperatures, which were maintained by resistive heating.[10] Whereas ΔL remained unchanged, we observed a non-linear relationship between the unfolding force and the temperature (Section S6 and Figure S5), which is consistent with previous studies.[11] Next, using this calibrated F_{unfold}–T relationship, we determined the temperature at different locations around the BOAT module by measuring F_{unfold} of the DNA hairpin at each position (Figure 2a and b). The accuracy of this temperature measurement was validated by the fact that the observed temperature profile is in good agreement with the theoretical prediction (Figure 2b), $T_{(r)} = T_{(0)} - Q/4\pi\kappa r$, where $T_{(0)}$ and $T_{(r)}$ are the temperatures at the particle surface and at a distance r, respectively, Q is the heat dissipated from the BOAT, and κ is the thermal conductivity of the medium.[7] Our results showed that when a 1 μm magnetic particle was illuminated by a 532 nm laser with a power of 10 mW, the temperature was 65 °C at the surface of the BOAT and 45 °C 1 μm away from the BOAT (Figure 2b). We also observed that the temperature at a particular location increased with the size of the magnetic particle or the power of the laser (Figure S6). For example, a 2.8 μm magnetic particle was able to induce a temperature of 45 °C 1 μm away from the BOAT using a 6 mW 532 nm laser. At laser powers of ≥ 15 mW (for a 1 μm magnetic particle) and ≥ 10 mW (for a 2.8 μm magnetic particle), temperatures can reach the boiling point of the medium as bubbles started to appear. These results suggest that the BOAT module is able to achieve T-jumps anywhere between ambient temperature and the boiling temperature of the medium in the range where most biochemical processes take place.

Next, we investigated the temporal resolution of the T-jump using the single-molecule thermometer. First, the folded state of the DNA hairpin was populated by clamping this molecule at 4 pN 1 μm away from the BOAT module (at 4 pN, k_{fold} and k_{unfold} are 0.58 s^{-1} and 6.2×10^{-6} s^{-1}, respectively; see Figure S7). When the BOAT was illuminated with a 10 mW 532 nm laser (Figure 2c, upper traces), the temperature increased to 43 °C, which led to unfolding of the hairpin at 4 pN ($F_{unfold} = 3.6 \pm 0.2$ pN at 43 °C). On the other hand, turning off the laser immediately refolded the hairpin. When we moved the hairpin 10 μm away from the BOAT or used a non-heating polystyrene particle as the BOAT, such unfolding–folding transitions (hopping) were not observed

(Figure 2c, lower traces), which confirmed that it was the temperature variation that changed the hopping behavior of the hairpin. Kinetic measurements revealed time constants of 5 ± 1 ms and 9 ± 1 ms (Figure 2d) for the heating and cooling T-jumps, respectively. As each transition involves two processes, the change in temperature and the unfolding or refolding of the hairpin at 4 pN, our measurements indicate that these values (5 and 9 ms) only represent the maximum response times for the T-jump. To determine the exact response time of the BOAT module, detectors with higher temporal resolutions and molecules with faster folding–unfolding transitions are required.

To confirm the temperature measurements by the mechanochemical thermometer and to demonstrate the potential of the BOAT module for microanalysis, we employed a thermosensitive polymer, poly(*N*-isopropylacrylamide) (PNIPAM), that undergoes a transition between insoluble (globular) and soluble (random coil) forms at the lower critical solution temperature (LCST).[12] We introduced an aqueous PNIPAM solution (1%; LCST = 32 °C) in a microfluidic channel and used a 1 μm magnetic particle as the BOAT (Figure 3a and b).

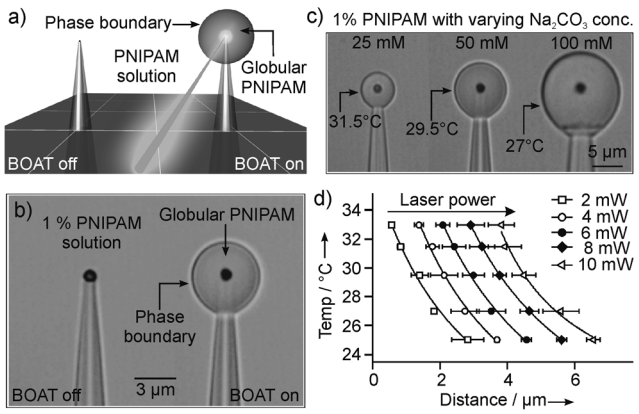

Figure 3. Temperature profile of the BOAT module measured by the phase transition of PNIPAM. a, b) Schematic representation (a) and microscope image (b) of the thermal gradient trap generated by the BOAT module that captures the PNIPAM-rich phase around the BOAT module. The phase boundary depicts the temperature equivalent to the LCST of the polymer. c) The size of the PNIPAM plume and the LCST vary with the ionic strength of the solution. d) The temperature profiles for different laser powers are in good agreement with the point-source steady-state heat transfer equation (——).

Within 30 ms after the 532 nm laser (8 mW) was turned on, insoluble PNIPAM particles appeared in a shadow of a sphere centered on the heated particle, which coalesced into a homogenous PNIPAM-rich plume around the BOAT module with a clear boundary against the surrounding medium. The plume reached an equilibrated size at approximately 15 s. Control experiments in the absence of BOAT or with the 532 nm laser focused on a non-heating polystyrene particle did not produce such a plume, which confirmed that the plume surrounding the BOAT was due to the temperature increase rather than the laser effect. When the heating laser was turned off, the PNIPAM-rich plume immediately dissolved within 60 ms because of the sudden and homogeneous decrease in temperature.

The clear interface between the PNIPAM plume and the aqueous solution represents the phase boundary that is defined by the LCST, which was determined to be 32.5 ± 0.5 °C by turbidity measurements. This observation allowed us to probe the temperature profile of the BOAT module by measuring the equilibrated position of the plume boundary. For this purpose, we mixed Na_2CO_3 (0–150 mM) into 1% PNIPAM solutions, which provided different LCSTs from 32.5 °C to 25 °C.[13] We performed two sets of experiments; either the power of the 532 nm laser was varied while using a solution with a particular Na_2CO_3 concentration, or the Na_2CO_3 concentration was changed while the laser power was kept the same (Figure 3c; see also Section S8 and Figures S10 and S11). By measuring the equilibrated (at ≥ 30 s) phase boundary position of the PNIPAM plume from these two sets of experiments, we obtained the temperature profile of the BOAT (Figure 3d; see also Section S8 and Figures S10 and S11). Although the size of the plume depends on the BOAT size (1 vs. 2.8 μm), the type of the BOAT material (magnetic vs. carbon), and the power of the 532 nm laser (2–10 mW), the temperature profile obtained here agreed well with that measured with the single-molecule thermometer (see also Section S8 and Figures S6 and S12).

Because of the efficient photothermal effect of a micrometer-sized black particle, a temperature gradient as steep as approximately 20 °C μm^{-1} has been established around the BOAT within milliseconds using a laser with a power as low as 6 mW (Figure S6), which is comparable to that of a hand-held laser pointer. This thermal gradient is approximately 20 times steeper than those achieved by traditional T-jump approaches.[14] The concept of heating through black microparticles may be extended beyond the BOAT setup. For example, similar T-jump profiles were obtained when a 2.8 μm black bead was placed on a glass surface (see also Section S9 and Figures S13 and S14). However, because of surface interference, the trapping of particles for mechanical force measurements becomes challenging. The microparticle in the BOAT not only allows easy integration into a lab-on-a-chip device, but also produces localized heat that minimizes thermal drift in optics. For force-based single-molecule experiments that require multiple optical components, the BOAT module provides an opportunity to carry out a rapid and large-scale temperature variation for the first time.

Unlike fluorescence-based thermosensors,[15] which suffer from background noise and succumb to photobleaching during the T-jump,[2] this mechanochemical thermometer hardly interferes with its environment as the system is isolated by the levitated particles. The use of low-intensity lasers and the avoidance of direct laser focusing on a sample drastically reduce the photodamage to the sample. The durability of the single molecule thermometer was demonstrated by the fact that despite of continuous illumination of the BOAT with the 532 nm laser for hours, unfolding and refolding transitions of the DNA hairpin were not compromised, even in a solution without an oxygen scavenging system.[5,9] A particular advantage of this single-molecule thermometry is the spatial resolution. For the DNA hairpin employed here, the tran-

sition between the folded and unfolded states occurs within a distance of 15 nm (Figure 2c and 4a). Given that the width and the length of the hairpin are 2 and 6 nm, respectively,[16] the volume in which the unfolding–refolding of this hairpin takes place is in the sub-yoctoliter range (0.2×10^{-24} L). Such a spatial resolution far surpasses that of most conventional temperature measurements that allow for in situ temperature measurements in single-molecule experiments. On the other hand, the temporal resolution and the temperature response range of the mechanochemical thermometer can be flexibly adjusted by using DNA hairpins with different unfolding and refolding rates.[9,17]

The advantages of our platform for single-molecule experiments have been well exploited in the investigation of the folding and unfolding processes of the same DNA hairpin at 23–43 °C. When we increased the temperature by moving the hairpin closer to the BOAT module, the force at which the probability of the folded and unfolded states is equal ($F_{1/2}$) decreased significantly while the hopping rate of the hairpin increased (Figure 4a). Fitting these hopping data to a two-state hidden Markov Model (HMM)[18] at various temperatures (Figure 4a) revealed that the unfolding and refolding transitions of the hairpin at $F_{1/2}$ were about 120 times faster with an increase of 20 °C in temperature (see also Table S2).

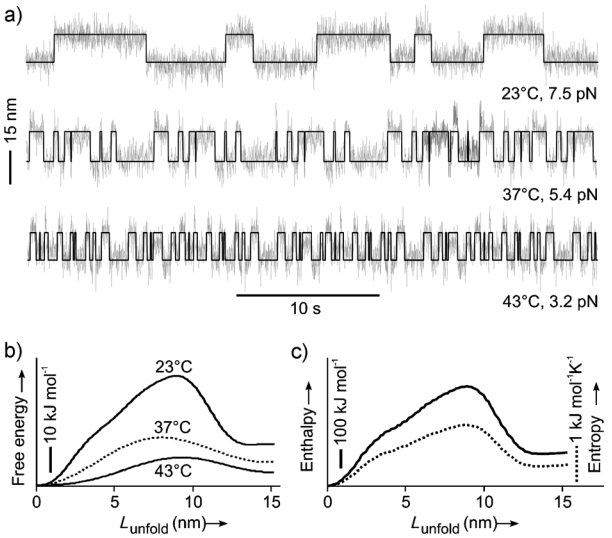

Figure 4. Transition dynamics of the DNA hairpin using the BOAT module and the mechanochemical thermometry. a) Extension–time traces for the DNA hairpin at a specific force and temperature at which folded and unfolded states are equally populated. The traces were fitted with a two-state hidden Markov Model.[18] b) Free-energy landscapes along the unfolding coordinate (L_{unfold}) of the DNA hairpin at 0 pN for various temperatures. c) Fully resolved unfolding landscapes of enthalpy (——) and entropy (•••••) of the same DNA hairpin at 0 pN. These landscapes are derived from the free-energy landscapes at four different temperatures (Section S7, Figures S8 and S9).

Next, we deconvoluted the folded and unfolded hairpin populations shown in Figure 4a using point spread functions (PSF; see also Section S7 and Figure S8).[9] Based on the Boltzmann distribution of these deconvoluted populations, we then retrieved the full unfolding free-energy (G_{unfold}) landscape of the hairpin at 0 pN from 23–43 °C (Figure 4b, see also Section S7 and Figure S8).[9] The accuracy of this approach has been validated by an excellent agreement of ΔG_{unfold} obtained from this treatment and that from conventional UV melting experiments (see also Section S7, Table S4, and Table S5). A comparison of these free-energy landscapes revealed that the energy barrier decreases with temperature, which is in full agreement with the changes in kinetic rates. Using the Gibbs–Helmholtz equation, we further calculated the change in unfolding enthalpy (ΔH_{unfold}) between a particular state along the coordinate (L_{unfold}) and the fully folded state, from which the change in entropy of unfolding (ΔS_{unfold}) was obtained (Section S7 and Figure S9). By setting the fully folded state as a reference point, ΔH_{unfold} and ΔS_{unfold} were then used to construct the unprecedented full unfolding enthalpy and entropy trajectories, respectively (Figure 4c). The shapes of all three thermodynamic trajectories look similar with maximum values around the transition state, which indicates that the folding of the DNA hairpin is enthalpy-driven throughout the whole process. Compared to previous mechanochemical studies that used force to manipulate the unfolding or refolding process of a biomolecule, our BOAT-integrated platform offers an additional dimension, namely temperature, to the system. This allows the multivariable description of a dynamic process using mechanical and thermal parameters (Figure 4a).

In summary, we have successfully combined two techniques, T-jump and single-molecule mechanical unfolding, to investigate the transition dynamics of biomolecules. By exploiting the highly efficient photothermal effect of black microparticles and the mechanochemical properties of a single DNA hairpin molecule, we have varied temperature within milliseconds and measured this variation within a yoctoliter volume. With this method, we were able to retrieve full landscapes of all of the three thermodynamic parameters, *G*, *H*, and *S*, for the unfolding transitions of a DNA hairpin. Phase transitions of a thermoresponsive polymer, PNIPAM, were also investigated in a microanalysis setting, demonstrating a potential application of this approach in lab-on-a-chip systems. Given the pivotal importance of temperature in various chemical, physical, and biological processes, we anticipate that this simple and generic BOAT platform integrated with single-molecule thermometry could offer new possibilities to understand these processes at the microscopic level.

Received: November 22, 2013
Revised: January 6, 2014
Published online: March 5, 2014

Keywords: mechanochemical properties · optical tweezers · single-molecule studies · temperature jump · thermometry

[1] J. Wang, D. Gan, L. A. Lyon, M. A. El-Sayed, *J. Am. Chem. Soc.* **2001**, *123*, 11284–11289; T. Hart, L. L. P. Hosszu, C. R. Trevitt, G. S. Jackson, J. P. Waltho, J. Collinge, A. R. Clarke, *Proc. Natl. Acad. Sci. USA* **2009**, *106*, 5651–5656; J. Kubelka, *Photochem. Photobiol. Sci.* **2009**, *8*, 499–512.

[2] R. Zhao, M. Marshall, E. A. Alemán, R. Lamichhane, A. Feig, D. Rueda, *Biophys. J.* **2010**, *99*, 1925 – 1931.
[3] X. S. Xie, R. C. Dunn, *Science* **1994**, *265*, 361 – 364; M. Rief, H. Clausen-Schaumann, H. E. Gaub, *Nat. Struct. Biol.* **1999**, *6*, 346 – 349; C. Bustamante, J. C. Macosko, G. J. L. Wuite, *Nat. Rev. Mol. Cell Biol.* **2000**, *1*, 130 – 136; W. J. Greenleaf, M. T. Woodside, S. M. Block, *Annu. Rev. Biophys. Biomol. Struct.* **2007**, *36*, 171 – 190.
[4] K. Jariashvili, B. Madhan, B. Brodsky, A. Kuchava, L. Namicheishvili, N. Metreveli, *Biopolymers* **2012**, *97*, 189 – 198; D. I. Pattison, A. S. Rahmanto, M. J. Davies, *Photochem. Photobiol. Sci.* **2012**, *11*, 38 – 53.
[5] M. P. Landry, P. M. McCall, Z. Qi, Y. R. Chemla, *Biophys. J.* **2009**, *97*, 2128 – 2136.
[6] C. M. Phillips, Y. Mizutani, R. M. Hochstrasser, *Proc. Natl. Acad. Sci. USA* **1995**, *92*, 7292 – 7296; R. M. Ballew, J. Sabelko, M. Gruebele, *Nat. Struct. Mol. Biol.* **1996**, *3*, 923 – 926.
[7] G. Kucsko, P. Maurer, N. Yao, M. Kubo, H. Noh, P. Lo, H. Park, M. Lukin, *Nature* **2013**, *500*, 54 – 58.
[8] M. K. Beyer, H. Clausen-Schaumann, *Chem. Rev.* **2005**, *105*, 2921 – 2948; M. M. Caruso, D. A. Davis, Q. Shen, S. A. Odom, N. R. Sottos, S. R. White, J. S. Moore, *Chem. Rev.* **2009**, *109*, 5755 – 5798; A. L. Black, J. M. Lenhardt, S. L. Craig, *J. Mater. Chem.* **2011**, *21*, 1655 – 1663; H. T. Baytekin, B. Baytekin, B. A. Grzybowski, *Angew. Chem.* **2012**, *124*, 3656 – 3660; *Angew. Chem. Int. Ed.* **2012**, *51*, 3596 – 3600; K. M. Wiggins, C. W. Bielawski, *Angew. Chem.* **2012**, *124*, 1672 – 1675; *Angew. Chem. Int. Ed.* **2012**, *51*, 1640 – 1643.
[9] M. T. Woodside, W. M. Behnke-Parks, K. Larizadeh, K. Travers, D. Herschlag, S. M. Block, *Proc. Natl. Acad. Sci. USA* **2006**, *103*, 6190 – 6195; D. Koirala, Z. Yu, S. Dhakal, H. Mao, *J. Am. Chem. Soc.* **2011**, *133*, 9988 – 9991.
[10] P. Luchette, N. Abiy, H. Mao, *Sens. Actuators B* **2007**, *128*, 154 – 160.
[11] R. Law, G. Liao, S. Harper, G. Yang, D. W. Speicher, D. E. Discher, *Biophys. J.* **2003**, *85*, 3286 – 3293.
[12] M. Heskins, J. E. Guillet, *J. Macromol. Sci.* **1968**, *2*, 1441 – 1455; H. G. Schild, *Prog. Polym. Sci.* **1992**, *17*, 163 – 249; C. Wu, X. Wang, *Phys. Rev. Lett.* **1998**, *80*, 4092 – 4094.
[13] Y. Zhang, S. Furyk, D. E. Bergbreiter, P. S. Cremer, *J. Am. Chem. Soc.* **2005**, *127*, 14505 – 14510.
[14] H. Kato, T. Nishizaka, T. Iga, K. J. Kinosita, S. Ishiwata, *Proc. Natl. Acad. Sci. USA* **1999**, *96*, 9602 – 9606; D. Braun, A. Libchaber, *Phys. Rev. Lett.* **2002**, *89*, 188103; H. Mao, J. R. Arias-Gonzalez, B. Smith, I. J. Tinoco, C. Bustamante, *Biophys. J.* **2005**, *89*, 1308 – 1316.
[15] J. Lou, T. M. Finegan, P. Mohsen, T. A. Hatton, P. E. Laibinis, *Rev. Anal. Chem.* **1999**, *18*, 235 – 284; Y. Shiraishi, R. Miyamoto, X. Zhang, T. Hirai, *Org. Lett.* **2007**, *9*, 3921 – 3924; D. Cauzzi, R. Pattacini, M. Delferro, F. Dini, C. Di Natale, R. Paolesse, S. Bonacchi, M. Montalti, N. Zaccheroni, M. Calvaresi, *Angew. Chem.* **2012**, *124*, 9800 – 9803; *Angew. Chem. Int. Ed.* **2012**, *51*, 9662 – 9665.
[16] R. R. Sinden, *DNA Structure and Function*, Academic Press, San Diego, CA, **1995**.
[17] A. Porchetta, A. Vallée-Bélisle, K. W. Plaxco, F. Ricci, *J. Am. Chem. Soc.* **2012**, *134*, 20601 – 20604.
[18] S. A. McKinney, C. Joo, T. Ha, *Biophys. J.* **2006**, *91*, 1941 – 1951; Y. Gao, S. Zorman, G. Gundersen, Z. Xi, L. Ma, G. Sirinakis, J. E. Rothman, Y. Zhang, *Science* **2012**, *337*, 1340 – 1343.

